Performance assessment of solar chimney power plants with the impacts of divergent and convergent chimney geometry

Erdem Cuce[1,2,*], Abhishek Saxena[3], Pinar Mert Cuce[2,4], Harun Sen[1,2], Shaopeng Guo[5] and K. Sudhakar[6,7,8]

[1]Department of Mechanical Engineering, Faculty of Engineering, Recep Tayyip Erdogan University, Zihni Derin Campus, Rize 53100, Turkey; [2]Low/Zero Carbon Energy Technologies Laboratory, Faculty of Engineering, Recep Tayyip Erdogan University, Zihni Derin Campus, Rize 53100, Turkey; [3]Department of Mechanical Engineering, Moradabad Institute of Technology, Moradabad 244001, India; [4]Department of Energy Systems Engineering, Faculty of Engineering, Recep Tayyip Erdogan University, Zihni Derin Campus, Rize 53100, Turkey; [5]College of Environment and Energy, Inner Mongolia University of Science and Technology, Bao Tou, Inner Mongolia 014010, PR China; [6]Faculty of Mechanical and Automobile Engineering Technology, Universiti Malaysia Pahang, Pahang 26600, Malaysia; [7]Energy Centre, Maulana Azad National Institute of Technology, Bhopal 462003, India; [8]Department of Electric Stations, Grids, and Power Supply systems, South Ural State University, Chelyabinsk 454080, Russian Federation

Abstract

Influence of area ratio (AR) on main performance parameters of solar chimney power plants (SCPPs) is investigated through a justified 3D axisymmetric CFD model. Geometric characteristics of Manzanares pilot plant (MPP) are taken into consideration for the numerical model. AR is varied from 0.5 to 10 to cover both concave and convex (convergent and divergent) solar chimney designs. Following the accuracy verification of the CFD results and proving mesh-independent solution, main performance oriented parameters are assessed as a function of AR such as velocity, temperature and pressure distribution within MPP, temperature rise of air in collector, mass flow rate of air around the turbine area, dynamic pressure difference across the turbine, minimum static pressure in the entire plant, power output and system efficiency. The results reveal that AR plays a vital role in performance figures of MPP. Mass flow rate of air ($\dot{m}$) is found to be 1122.1 kg/s for the reference geometry (AR = 1), whereas it is 1629.1 kg/s for the optimum AR value of 4. System efficiency (η) is determined to be 0.29% for the reference case; however, it is enhanced to 0.83% for the AR of 4.1. MPP can generate 54.3 kW electrical power in its current design while it is possible to improve this figure to 168.5 kW with the optimal AR value.

Keywords: solar chimney; divergent and convergent chimney; maximum velocity; power output; system efficiency; chimney design

*Corresponding author: erdemcuce@gmail.com

Received 12 November 2020; revised 1 December 2020; editorial decision 8 December 2020; accepted 8 December 2020

International Journal of Low-Carbon Technologies 2021, 16, 704–714

https://doi.org/10.1093/ijlct/ctaa097 Advance Access publication 22 January 2021

1. INTRODUCTION

Industrial developments over the past century have undoubtedly facilitated human life. However, they have also caused some serious matters such as global warming, uncontrolled CO_2 emissions and environmental pollution. Especially the fact that the attempts to reduce CO_2 emissions did not yield the desired levels and rapidly rising human population worldwide have pushed scientists to seek alternative clean energy technologies. Renewable energy technologies have been in the focal point of research activities notably over the past four decades owing to eco-friendly feature of these systems as well as abundance of natural energy resources. Solar energy, which is one of the renewable energy sources, can be used anywhere regardless of location on Earth and has a great potential. Solar energy systems can be designed as a direct or indirect energy harnessing unit, and they are mostly utilized for the purposes of thermal and electrical energy production. While the solar thermal energy can be used directly with simple mechanisms, some systems need to be installed to obtain electrical energy. One of the said systems for solar assisted electricity generation is solar chimney power plants (SCPPs) [1]. Solar chimneys (SCs) are renewable energy-based power plants, which are driven by two main physical principles. The first is the upward movement of the heated air due to the density difference, and the second is the rising momentum of air due to the pressure difference between chimney inlet and outlet [2].

SCPPs consist of three main parts (collector, chimney and turbine) [3]. The first part is the collector where the solar energy is collected and harnessed to increase the thermal energy content of air flowing within the system. This part, which is a transparent or translucent cover, enables the sun rays to reach the air and the ground in the plant. Solar radiation reaching the ground is somewhat stored within ground material as heat and yields to a temperature increase. This temperature rise enables lifting effects in the air, which is a driving force for the operation of SCs [4]. The other two parts are the chimney and the turbine. When a high chimney with circular cross-section is fixed in vertical position, pressure difference occurs due to elevation difference at the entrance and exit. This pressure difference causes constant upward physical movement of air near the ground of the chimney [5]. Since this physical movement is independent of the sun, SCPPs can continue to be active in the hours when there is no sun and generate electricity at a certain efficiency range. The system air, which is partially heated under the collector as a consequence of greenhouse effect and is exposed to buoyant forces, moves upwards by entering the vertically located chimney in the collector centre. Electricity is produced in the system by rotating the turbine placed at a certain height from the chimney ground.

The theory of SCPPs was first introduced in the early 1900s. However, the first successful application was built in Manzanares, Spain, in 1982. The first experimental attempts on Manzanares pilot plant (MPP) have been carried out by Haaf [6]. Main performance parameters and efficiency figures have been first proposed in the said pioneer work through an experimental methodology. In the following years, theoretical and numerical approaches have been adopted for performance assessment of MPP as a function of geometric parameters. For instance, Mullet [7] has determined the temperature, velocity and efficiency figures of MPP for different geometrical designs. It has been illustrated that a power output of 1000 MW can be obtained with a chimney diameter of 400 m and a chimney height of 900 m. Corresponding system efficiency for the said design is reported to be 1%. Impacts of environmental parameters such as solar radiation and ambient temperature on the performance figures of MPP have also been discussed through theoretical and numerical works. Previous works have indicated that power output of SCPPs increases with the incoming solar intensity [8–10]. On the other hand, power output has been observed to decrease with ambient temperature [11].

The change in geometric parameters has different effects on the performance outputs of SCPPs. For example, increasing the height of the chimney yields to linear enhancement in the power output of the system [12, 13], and a similar tendency is noticed for the collector radius [14]. However, it has been reported in previous works that the power output does not show a noticeable change after a certain value of collector radius [15]. Remarkable impact of chimney geometry on electricity generation efficiency has stimulated researchers to conduct theoretical and numerical analyses for SCPPs. As an example, Choi et al. [16] have analysed the 24-hour performance of MPP with an analytical model they developed. They have showed that the results of the analytical model are consistent with the experimental data. Afterwards, they have examined the effects of geometric parameters, energy storage system and climatic conditions on the performance of SCPPs. They have also made a performance estimation for a certain design of SCPP with 1000 m chimney height, 100 m chimney radius, 3000 m collector radius, 5 m collector inlet height and 25 m collector outlet height. They have stated that the power output is 40 MW when the chimney diameter is 50 m. On the other hand, the power output reaches 150 MW for the chimney diameter of 150 m. Toghraie et al. [17] have developed a 3D axisymmetric CFD model for SCPPs to evaluate the influence of geometric parameters on the performance figures. For a system design with 100 m chimney height, 4 m chimney radius, 100 m collector radius and 2 m collector height, efficiency and power output values have been determined as a function of geometric parameters. They have demonstrated that there is a linear relationship between chimney height and power output as well as system efficiency. On the other hand, it has been reported that the situation is totally different in terms of the impacts of chimney diameter. Mass flow rate, pressure difference, power output and efficiency figures are enhanced up to a certain value of chimney diameter, but then they all show a decreasing tendency. For a solar intensity of 800 W/m^2, power output and efficiency of the plant has been determined to be 80 kW and 0.31%, respectively. When the chimney diameter is increased to 10 m, power output reaches 86 kW and system efficiency 0.32%, which needs to be noted. Hassan et al. [18] have investigated the effects of collector and chimney slopes on system performance. A 3D CFD model has been developed for MPP in which RNG k-ε turbulence model and discrete ordinate (DO) radiation model are adopted. They have reported that the air flow

rate in the system is enhanced by the increase in collector slope. However, after 6° collector slope, air flow is deteriorated and the system performance is observed to be negatively affected. It has been also underlined that the rise in chimney slope improves the performance parameters of MPP. For a chimney slope of 1°, power output is found to increase 108% through the enhancement in maximum velocity values from 9.1 to 11.6 m/s. The results have proved that greater power outputs can be achieved with smaller chimney heights and collector radii when optimum slope configurations are taken into consideration.

The ratio of chimney outlet area to the chimney inlet area (AR) has been investigated by several researchers to date for different SCPP designs. Hu et al. [19] have examined this impact for 3 different chimney heights and 32 different AR values. Temperature and velocity profiles as well as power output have been determined as a function of AR. The results have revealed that power output of a SC rises with increasing AR, it starts to decrease but after a certain value of AR. The simulations conducted for MPP reveal that power output can be enhanced more than 13 times for AR = 10. It has been also emphasized that the optimum AR value is a function of chimney height. Koonsrisuk and Chitsomboon [20] have developed a 5° axisymmetric CFD model to study the effects of chimney outlet area on SCPPs. Velocity and mass flow rate of air, temperature and pressure distributions and power output values have been obtained for a SCPP system with 100 m chimney height, 2 m collector height, 100 m collector radius and 4 m chimney inlet radius. They have stated that the velocity and mass flow rate figures of the system are improved with the rising AR. They have also claimed that when the output radius is 16 m, the mass flow rate increases 4.5 times and the power output 94.29 times according to the reference case.

It is understood from the literature survey that SCPPs have been investigated to date through theoretical, experimental and numerical works. Especially MPP has been considered in the analyses with its geometric parameters since it refers to the first successful application of SCs in the world. When studies conducted in recent years on SCPPs are analysed, it is seen that CFD-based studies are in the majority since they enable to examine the geometric and environmental parameters for a system simultaneously. Most of the CFD analyses merely focus on evaluating a limited number of independent variables on system performance figures. Chimney height and collector radius are frequently studied; however, chimney design and AR impact are rarely investigated despite their remarkable role in power output and system efficiency. Therefore, this research aims at examining the influence of AR on main performance parameters of MPP such as relative pressure difference near the turbine, temperature distribution along the collector, mass flow rate and maximum velocity of air, system efficiency and available power output.

2. METHODOLOGY

2.1. Governing equations

In the present research, the chimney inlet radius is kept constant and the outlet radius is varied for the AR values in the range of $0 < AR < 1$ and $AR > 1$ representing both the convergent and divergent chimney design. By doing so, possible influence of different AR configurations on performance parameters of SCPPs is evaluated for the characteristic geometric and environmental properties of MPP. By coupled solving of continuity, momentum, energy and turbulence model equations, regression equations are achieved for mass flow rate, maximum velocity, pressure difference, collector outlet temperature, system efficiency and power output. The assumptions made to simplify the analysis are as follows:

—The air inside the system is considered incompressible.
—Flow is considered constant, 3D and turbulent.
—Environmental conditions are assumed constant.
—Boussinesq model is accepted for density change of air.

Continuity equation:

$$\frac{\partial \rho}{\partial t} + \frac{\partial (\rho u)}{\partial x} + \frac{\partial (\rho v)}{\partial y} + \frac{\partial (\partial w)}{\partial z} = 0 \tag{1}$$

Momentum equation:

$$\frac{\partial (\rho u)}{\partial t} + \frac{\partial (\rho uu)}{\partial x} + \frac{\partial (\rho uv)}{\partial y} + \frac{\partial (\rho uw)}{\partial z} = -\frac{\partial p}{\partial x} + \mu \left(\frac{\partial^2 u}{\partial x^2} + \frac{\partial^2 u}{\partial y^2} + \frac{\partial^2 u}{\partial z^2} \right) \tag{2}$$

$$\frac{\partial (\rho v)}{\partial t} + \frac{\partial (\rho vu)}{\partial x} + \frac{\partial (\rho vv)}{\partial y} + \frac{\partial (\rho vw)}{\partial z} = -\frac{\partial p}{\partial y} + \mu \left(\frac{\partial^2 v}{\partial x^2} + \frac{\partial^2 v}{\partial y^2} + \frac{\partial^2 v}{\partial z^2} \right) \tag{3}$$

$$\frac{\partial (\rho w)}{\partial t} + \frac{\partial (\rho wu)}{\partial x} + \frac{\partial (\rho wv)}{\partial y} + \frac{\partial (\rho ww)}{\partial z} = -\frac{\partial p}{\partial z} + \mu \left(\frac{\partial^2 w}{\partial x^2} + \frac{\partial^2 w}{\partial y^2} + \frac{\partial^2 w}{\partial z^2} \right) + \rho g \beta (T - T_a) \tag{4}$$

Energy equation:

$$\frac{\partial (\rho cT)}{\partial t} + \frac{\partial (pcuT)}{\partial x} + \frac{\partial (pcvT)}{\partial y} + \frac{\partial (pcwT)}{\partial z} = \lambda \left(\frac{\partial^2 T}{\partial x^2} + \frac{\partial^2 T}{\partial y^2} + \frac{\partial^2 T}{\partial z^2} \right) \tag{5}$$

In SCPPs, natural convection takes place within the entire system. The Rayleigh number for the natural convection process within SCs can be given by:

$$Ra = \frac{g \beta \Delta T {H_c}^3}{\alpha \upsilon} \tag{6}$$

where H_c is the collector height, α is the thermal diffusion coefficient and ν is the kinematic viscosity. Within the present work, *Ra* number is found to be highly greater than critical value of 10^9, and thus the flow is considered to be turbulent [21]. There are three different turbulence models used in the analysis of SCPPs in literature. Some researchers prefer to use standard k-ε turbulence model, which is practical, is accurate in many flows and does not depend on flow regime and geometry [21–23]. On the other hand, realizable k-ε turbulence model is adopted in some works depending on geometric characteristics [19, 24]. In this research, RNG k-ε turbulence model is utilized, which is much more appropriate for turbulent flows with strong swirl and vortex effects [10]. Turbulence model equations can be given as follows:

$$\frac{\partial}{\partial t}(\rho k)+\frac{\partial}{\partial x_i}(\rho k u_i)=\frac{\partial}{\partial x_j}\left[\alpha_k \mu_{eff}\frac{\partial k}{\partial x_j}\right]+G_k+G_b+\rho\varepsilon-Y_M+S_k \tag{7}$$

$$\frac{\partial}{\partial t}(\rho\varepsilon)+\frac{\partial}{\partial x_i}(\rho\varepsilon u_i)=\frac{\partial}{\partial x_j}\left[\alpha_\varepsilon \mu_{eff}\frac{\partial \varepsilon}{\partial x_j}\right] + C_{1_\varepsilon}\frac{\varepsilon}{k}(G_k+C_{3\varepsilon}G_b)-C_{2\varepsilon}\rho\frac{\varepsilon^2}{k}-R_e+S_\varepsilon \tag{8}$$

In SCPPs, Boussinesq model is usually preferred to calculate the density change of air within the system depending on temperature. Boussinesq model can be expressed as follows:

$$(\rho-\rho_a)\,g \approx -\rho_a \beta\,(T-T_a)\,g \tag{9}$$

In the said equation, β is the thermal expansion coefficient, ρ_a is the density and T_a is the temperature of inlet air. The thermal energy input to the SCPP is supplied by the collector part. This energy can be given by the following equation:

$$\dot{Q}=\dot{m}C_p\Delta T \tag{10}$$

In this equation, ΔT refers to the temperature rise in the collector from inlet to outlet. Collector efficiency can also be calculated by dividing $\dot{Q}$ to the total energy falling on collector surface as follows:

$$\eta_{coll}=\frac{\dot{Q}}{A_{coll}G} \tag{11}$$

where A_{coll} is the total collector area and G is the incoming solar radiation. There are different approaches in literature for the calculation of power output. In most cases, power output is determined through the pressure drop across the turbine (ΔP_t) [10, 24] as follows:

$$P_o=\eta_t \Delta P_t Q_v \tag{12}$$

In this equation, η_t is the turbine efficiency, and it is taken to be 0.8 in most cases [10, 19, 24, 25]. It is understood from the equation that pressure drop and volumetric flow rate (Q_v) are the two main parameters affecting the power output of a SCPP [25]. There are also different methods in literature to determine ΔP_t. The present work aims to specify ΔP_t via the average pressure (P_t) at the turbine position based on the findings through CFD research. The said approach can be given as follows:

$$\Delta P_t = r_t\, P_t \tag{13}$$

In this equation, r_t is the turbine pressure drop ratio, and taken to be 2/3 [12]. Overall system efficiency for a SCPP is given by

$$\eta=\frac{P_o}{A_{coll}G} \tag{14}$$

Table 1. *Geometric characteristics of MPP in Spain.*

Geometric parameter	Value
Mean collector radius	122.0 m
Mean collector height	1.85 m
Chimney height	194.6 m
Chimney radius	5.08 m
Ground thickness	0.5 m
Area ratio (AR)	0.5 ÷ 10

2.2. Parametric research

Within the scope of this parametric research, simulations are conducted by taking MPP into consideration, which is the first successful example of SCPP systems. Geometric data and configuration details of the system are given in Table 1 [5]. Previous experimental attempts reveal that the temperature does not change with time from 0.5 m below the ground, hence the ground thickness is taken as 0.5 m in the CFD simulations [6, 10]. As previously notified, the ratio of chimney outlet area to the chimney inlet area is defined as area ratio (AR), and the numerical calculations are repeated for the AR values from 0.5 to 10 for their potential impact of main performance parameters.

2.3. CFD analysis

There are different approaches based on finite volume method in literature for numerical performance assessment of SCPPs. When the said works are evaluated, it is understood that some researchers use 2D axisymmetric models [19, 25], whereas some prefer 3D CFD models for a more accurate, reliable and scientific approach [21–23]. Similar to them, a 3D axisymmetric CFD model is proposed in this study for a precise analysis of flow characteristics in MPP. The model geometry is constructed in ANSYS WORKBENCH, which is ideal for such a research. In the previous works, it is also noticed that a certain fraction of whole system is considered in the analyses to expedite the iteration process. For instance, Hassan et al. [18] prefer to use a 180° CFD model, whereas a 5° model is adopted by Koonsrisuk and Chitsomboon [20]. In this research, a 90° CFD model is developed for the MPP sketch given in Figure 1, and the analyses are repeated following

Table 2. *Mesh-independent solution for the reliability of the CFD research.*

Cell count	$\dot{m}$	V_m	P_o	% chg. in $\dot{m}$	% chg. in V_m	% chg. in P_o
258 385	1118.2168 kg/s	14.0379 m/s	54465.05556 W	—	—	—
310 576	1124.1816 kg/s	14.1296 m/s	54568.94209 W	0.533	0.653	0.190
388 177	1117.9028 kg/s	14.20285 m/s	54333.95226 W	0.558	0.518	0.430

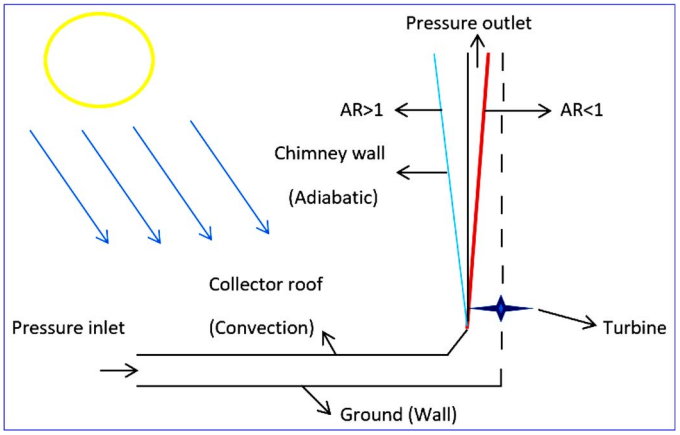

Figure 1. *Convergent and divergent chimney impact for the case of Manzanares solar chimney pilot plant.*

Table 3. *Main parameters considered in CFD modelling.*

Solar radiation (W/m^2)	1000
Ambient pressure (Pa)	101325
Ambient temperature (K)	293.15
Gravitational acceleration (m/s^2)	9.81
Ambient air density (kg/m^3)	1.2046
Ideal gas constant (J/kgK)	287
Air conductivity (W/mK)	0.0259
Kinematic viscosity of air (m^2/s)	1.48×10^{-5}
Air heat capacity (J/kgK)	1006.43
Stefan–Boltzmann constant (W/m^{2}K^4)	5.667×10^{-8}
Turbine pressure drop ratio	2/3

the accuracy justification of mesh-independent solution. The proposed model includes two plane symmetries (XZ and YZ planes). Triangular mesh cells are preferred in the research due to intensive curvatures. Through the findings of mesh-independent solution listed in Table 2, the CFD analyses are carried out for the cell count of 388177. RNG k-ε turbulence model is utilized for the solution of momentum equation. DO non-grey radiation integrated with solar ray tracing approach is adopted. SIMPLE algorithm is used to assess the interaction between pressure and velocity figures. Change of air density by temperature is evaluated through Boussinesq approximation. Convergence criterion is selected to be 10^{-6} for each parameter, which is acceptable for such a research. Essential parameters utilized in CFD modelling are presented in Table 3.

Table 4. *Physical properties of the materials used in the CFD research.*

Physical property (unit)	Glass	Ground	Chimney
Density (kg/m^3)	2500	2160	2719
Thermal conductivity (W/mK)	1.15	1.83	202.4
Specific heat (J/kgK)	750	710	871
Absorption coefficient	0.03	0.9	0
Transmissivity	0.9	Opaque	Opaque
Emissivity	0.1	0.9	1
Refractive index	1.526	1	1
Thickness (m)	0.004	0.5	0.00125

3. RESULTS AND DISCUSSION

In the present research, the chimney inlet radius is kept constant and the outlet radius is varied for the AR values in the range of 0.5–10 in order to cover both concave and convex chimney geometry. Parametric research is carried out according to the geometric characteristics of MPP. The CFD model is structured in ANSYS WORKBENCH, which gives reliable and realistic performance results in similar works. Pressure inlet boundary condition is set at the collector inlet and pressure outlet is adopted at the chimney outlet. For chimney wall, ground and collector, boundary condition is specified as wall. It is assumed that no heat loss takes place through chimney wall and ground ($h = 0\ W/m^2K$), whereas natural convection is available within the air medium beneath the collector with a convection coefficient of $h = 10\ W/m^2K$. In addition, chimney and ground are considered to be opaque in the CFD analyses while collector is semi-transparent. Physical properties of the materials utilized in the modelling are listed in Table 4.

CFD analyses in the present work are performed for a cell count of 388 177 as a consequence of the mesh-independent solution. Accuracy justification of the preliminary findings is done through the previous experimental and numerical analyses conducted for MPP. Maximum velocity (V_m) in the SCPP is a main performance indicator, thus most of the researchers attempt to verify the reliability of CFD findings over this term. Figure 2 illustrates the V_m values for different solar intensity levels. It is clear from the results that the present work is in good accordance with the experimental data [26] and surpasses the previous numerical attempts [14]. For the solar intensity of 800 W/m^2, experimental V_m is reported to be 12 m/s. Ming et al. [14] propose a numerical V_m of 14.64 m/s for the said solar intensity, whereas it is found to be 13.1 m/s in the present work, which proves the reliability of the CFD methodology adopted in this study.

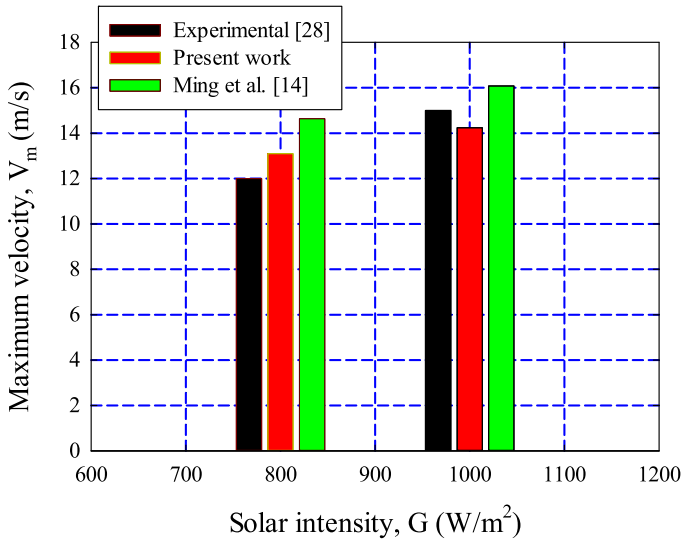

Figure 2. *Accuracy verification of the CFD research through a case study for MPP.*

Pressure at the turbine inlet is a significant performance parameter in the feasibility analyses of SCPPs. The lower pressure values the higher velocity figures around the turbine, hence accurate determination of static contours of pressure is of vital importance for realistic interpretation of the CFD findings. In order to illustrate the impacts of concave chimney geometry on static contours of pressure around the turbine inlet, three different cases are taken into consideration (AR = 0.50, 0.75 and 1) as shown in Figure 3. At first glance, it is understood that pressure values decrease with increasing AR, which means greater mass flow rates thus air velocities within the plant. Relative pressure differences somewhat rise from centre to the chimney wall at the section in which the turbine is fixed [27]. Minimum pressure values are reported to be −45.3, −80.1 and −113.4 Pa for AR = 0.5, 0.75 and 1, respectively.

A similar scenario takes place for the convex chimney geometry. According to the static contours of pressure achieved for the AR values of 1, 2.5 and 5, it is observed that relative pressure differences are enhanced with the rise in AR value as depicted in Figure 4. Somewhat lower pressure values are noticed toward the chimney wall. For AR = 1, 2.5 and 5, minimum pressure values are determined to be −113.4, −218.2 and −233.8 Pa, respectively. Divergent chimney geometry enables greater volumes of air to enter the turbine section, which yields to remarkable improvements in mass flow rates thus air velocities. However, it is well known that mass flow rate is also affected by buoyant forces associated with temperature and pressure distributions along the collector and around the chimney inlet. The aforesaid effects are considerably driven by the divergent chimney geometry as a function of AR. In this respect, there should be an optimum value of AR for optimum mass flow rate, pressure difference and power output for MPP and any type of SCPP.

Temperature distribution within the collector is of significant relevance to the power output of SCPPs due to its notable influence on mass flow rate of air entering the turbine. As the first step, static contours of temperature are produced for the AR values of 0.50, 0.75 and 1 as depicted in Figure 5. It is observed from the findings that temperature rise in the collector is a considerable function of AR. Maximum temperature for AR = 0.5 is obtained at the collector outlet as 306.4 K while it is 304.5 and 303.2 K for the AR of 0.75 and 1, respectively. The reduction in maximum collector temperature can be attributed to the limited energy input to the air medium with increasing AR since the mass flow rate figures are notably enhanced with the rise in AR. A similar scenario takes place for the convex chimney geometry as shown in Figure 6.

According to the static contours of temperature achieved for the AR values of 1, 2.5 and 5, maximum temperature within the collector at the outlet is determined to be 303.2, 301.2 and 300.8 K for AR = 1, 2.5 and 5, respectively. Collector temperatures reduce with increasing AR as the chimney geometry changes from concave to convex profile. Temperature of air flowing along the collector is also determined for the AR values in the range of 0.5–10 as given in Figure 7. By getting the geometric configurations and operational characteristics of MPP, a novel regression model is also developed for the first time in literature as follows:

$$T_a = 341.3 + \frac{-3875}{AR} \exp\left[-0.5\left(\frac{\ln\left(\frac{AR}{3052}\right)}{2.587}\right)^2\right] \qquad (15)$$

It is understood from the findings that AR dramatically affects the temperature rise in the collector. For the AR = 0.5, the greatest air temperature at the collector outlet is observed with 314.9 K. T_a is found reducing up to a certain value of AR, which is 3.75. For the AR value of 3.75, minimum temperature increase is observed for air with 305.2 K. From this point, T_a values show a steady rise up to AR = 10. For the greatest convex geometry, T_a is determined to be 307.7 K. When the static contours of temperature for the collector material are investigated, it can be easily concluded that the contour data are in good accordance with the air temperatures at the collector outlet. In MPP, temperature figures show a decreasing tendency from ground to the collector due to convection and radiation oriented heat losses.

Static contours of velocity throughout the concave and convex SC designs are also achieved within the present. Air velocities (V_a) for the AR values of 0.5, 0.75 and 1 are demonstrated in Figure 8. It is known for MPP that the turbine is placed 9 m above from the ground. From this point of view, velocity contours at the aforesaid section of chimney are of vital importance relative to the other parts of the SC. For the original dimensions of MPP, which corresponds to AR of 1, maximum air velocity around the turbine position is obtained to be 13.9 m/s for the solar intensity of 1000 W/m^2. For the lower values of AR, relatively lower velocity figures are achieved at the turbine position. This can be explained by the change in mass flow rate with AR. For the greater values

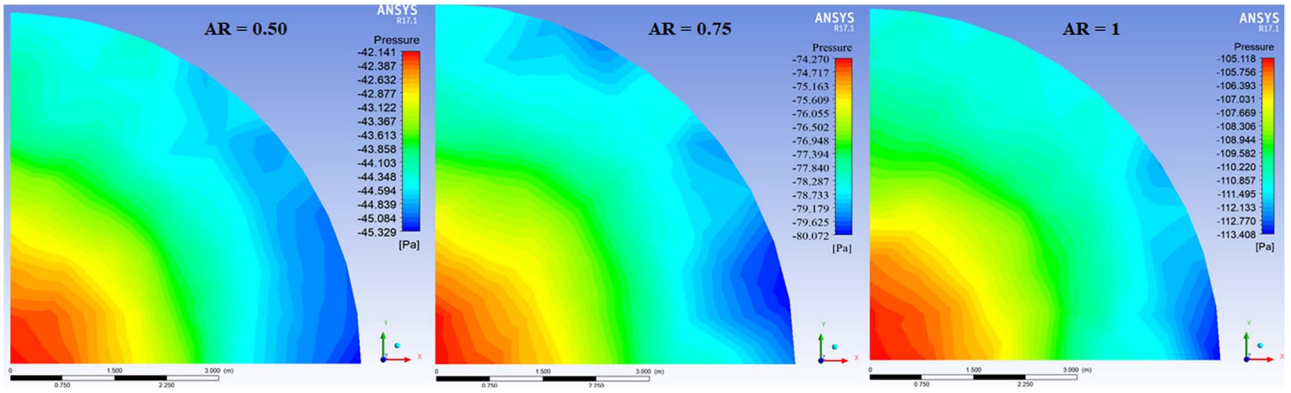

Figure 3. *Static contours of pressure near the turbine inlet for AR = 0.50, 0.75 and 1.*

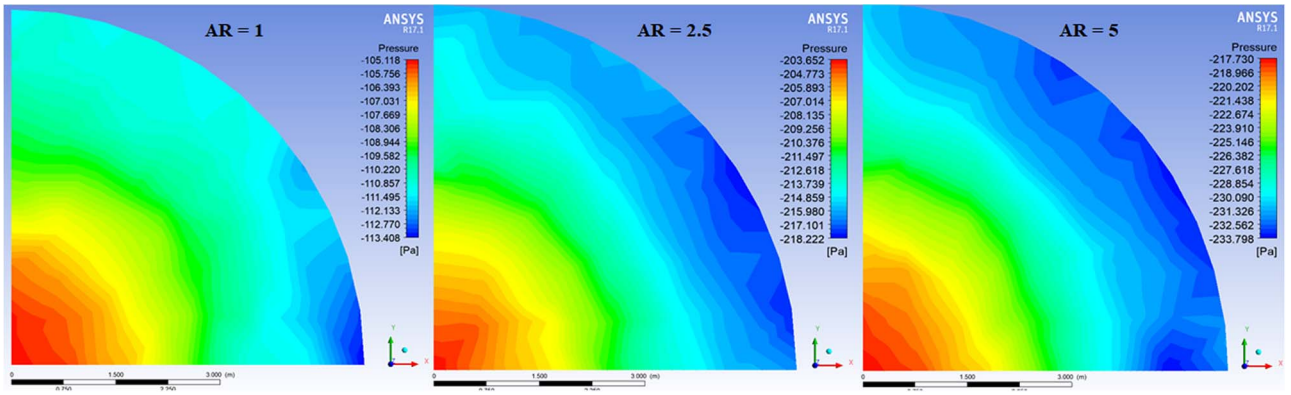

Figure 4. *Static contours of pressure near the turbine inlet for AR = 1, 2.5 and 5.*

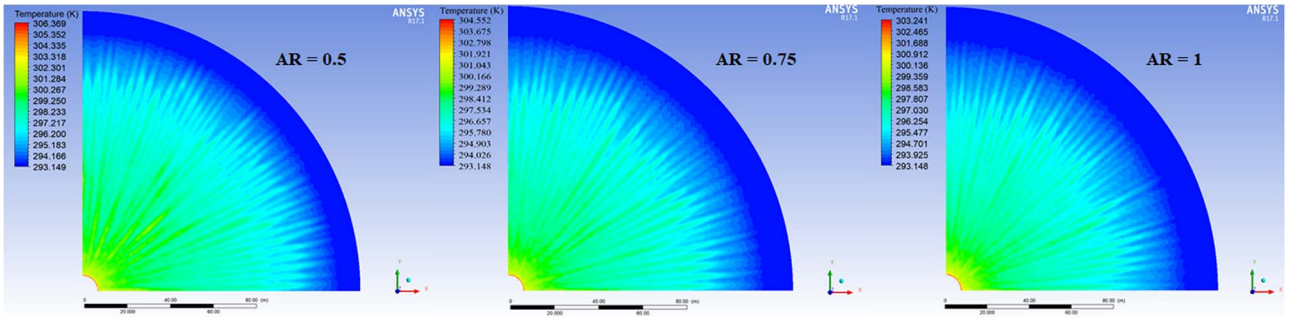

Figure 5. *Static contours of temperature along the collector for AR = 0.50, 0.75 and 1.*

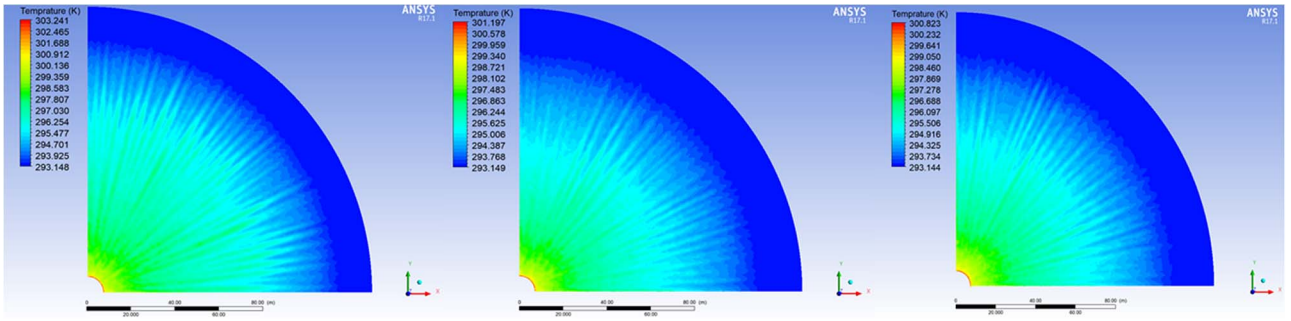

Figure 6. *Static contours of temperature along the collector for AR = 1, 2.5 and 5.*

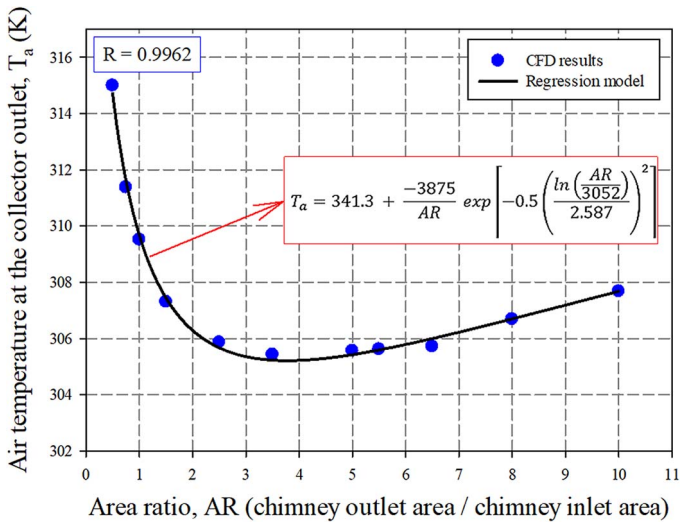

Figure 7. *Temperature increase of air at the collector outlet as a function of AR.*

of AR than 1 (convex geometry), mass flow rates are notably improved, which yields to higher V_a values around the turbine as shown in Figure 9. Maximum V_a is determined to be 19.1 and 19.8 m/s for the AR of 2.5 and 5, respectively.

Mass flow rate is a significant parameter for SCPPs due to its direct influence on power output. Therefore, $\dot{m}$ of air within the system is determined as a function of AR as depicted in Figure 10. It is understood from the findings that $\dot{m}$ sharply increases with AR up to a certain point, then shows a slight decrease till the final value of AR, which is considered as 10 in the present work. The AR value, which maximizes the $\dot{m}$, is found to be 4.3, and the corresponding $\dot{m}$ value is achieved to be 1629.1 kg/s. For the AR of 0.5 and 10, $\dot{m}$ is determined to be 735.7 and 1433.4 kg/s, respectively. For the actual geometric characteristics of MPP, which corresponds to the AR of 1, $\dot{m}$ is found to be 1122.1 kg/s. From this point of view, it can be easily concluded that divergent chimneys considerably improve the $\dot{m}$ figures of the plant. For the first time in literature, $\dot{m}$ is obtained as a function of AR through the following regression model:

$$\dot{m} = 105.9 + \frac{24100}{AR} \exp\left[-0.5\left(\frac{\ln\left(\frac{AR}{58.41}\right)}{1.616}\right)^2\right] \quad (16)$$

Another important performance parameter for SCPPs is the dynamic pressure difference across the turbine (ΔP_{dyn}). It is clear from the findings that ΔP_{dyn} exponentially decreases with AR up to a critical point and then gradually rises as shown in Figure 11. This critical point for the MPP is determined to be 4.1. Corresponding pressure at this point is achieved as −232.3 Pa. When the original geometry of MPP is taken into consideration (AR = 1), ΔP_{dyn} is found as −109.8 Pa. This finding justifies the positive influence of divergent chimney geometry on overall performance of MPP. Similar to the previous performance parameters, a regression analysis is carried out for ΔP_{dyn} as given below depending on AR:

$$\Delta P_{dyn} = \frac{-1872}{AR} \exp\left[-0.5\left(\frac{\ln\left(\frac{AR}{15.74}\right)}{1.159}\right)^2\right] \quad (17)$$

The minimum static pressure is also proposed within the present study as illustrated in Figure 12. For an AR value of 3.9, minimum pressure is observed within the entire plant with −386.6 Pa. For the actual geometry of MPP, which corresponds to the AR of 1, P_s is achieved as −181.7 Pa. Minimum static pressure (P_s) can be correlated with AR as given below:

$$P_s = \frac{-2799}{AR} \exp\left[-0.5\left(\frac{\ln\left(\frac{AR}{13.45}\right)}{1.113}\right)^2\right] \quad (18)$$

Figure 13 demonstrates the dependency of power output (P_o) on AR. For the reference geometry of MPP, P_o is found to be in good accordance with the experimental data. In the present work, P_o is determined to be 54.3 kW, whereas it is given 55 kW in the previous experimental analyses. It is also perspicuous from the CFD findings that AR plays a key role in P_o owing to its notable influence on $\dot{m}$ and ΔP_{dyn}. For the optimum value of AR (4.1), P_o is predicted to be 168.5 kW, which is noteworthy. For concave geometry of MPP (e.g. AR = 0.5), P_o is observed to reduce to 14.2 kW. However, for the convex geometry (e.g. AR = 10), P_o is still enhanced compared to the reference case with 108.9 kW. The following regression model is developed for the interaction between P_o and AR:

$$P_o = -2647 + \frac{1116000}{AR} \exp\left[-0.5\left(\frac{\ln\left(\frac{AR}{10.37}\right)}{0.9636}\right)^2\right] \quad (19)$$

System efficiency (η) is also evaluated within the present research as shown in Figure 14. For the reference geometry, η is determined to be 0.29%. However, η is found changing notably with AR for both concave and convex chimney geometry. For the optimum AR value of 4.1, η is predicted to be 0.83%, which corresponds to about 186% enhancement compared to the reference case. It is also concluded that concave geometries are not appropriate in terms of performance figures. For instance, η is determined to be 0.09% for AR = 0.5. Convex chimney designs give better performance in all cases in comparison to the standard geometry of MPP. For the AR of 6, 8 and 10, η is obtained to be 0.77, 0.67 and 0.56%, respectively. Finally, η is correlated with AR by the following regression model:

$$\eta = -0.008118 + \frac{5.725}{AR} \exp\left[-0.5\left(\frac{\ln\left(\frac{AR}{11.28}\right)}{1.004}\right)^2\right] \quad (20)$$

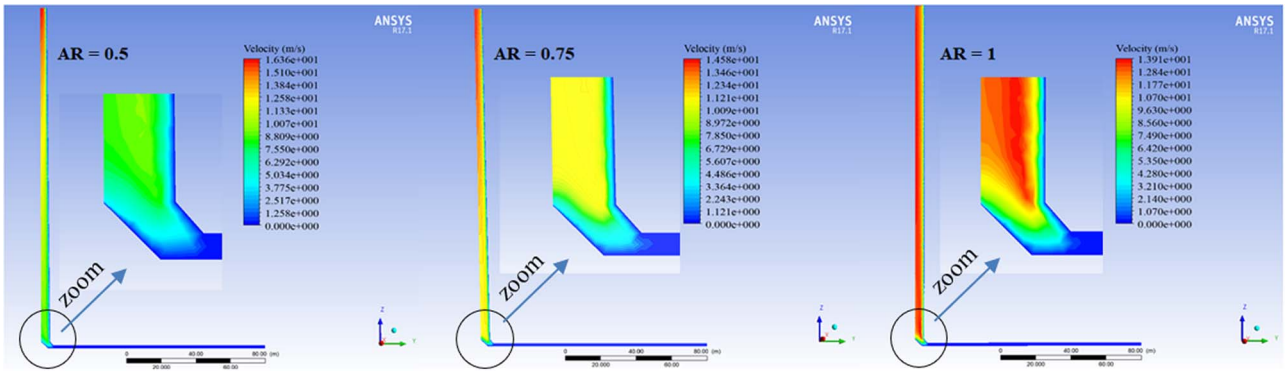

Figure 8. *Static contours of velocity throughout the SC for AR = 0.50, 0.75 and 1.*

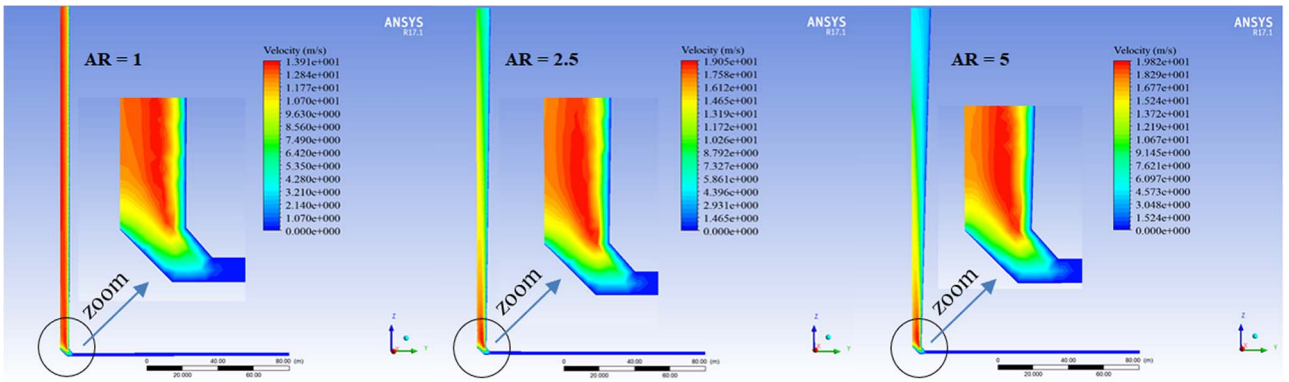

Figure 9. *Static contours of velocity throughout the SC for AR = 1, 2.5 and 5.*

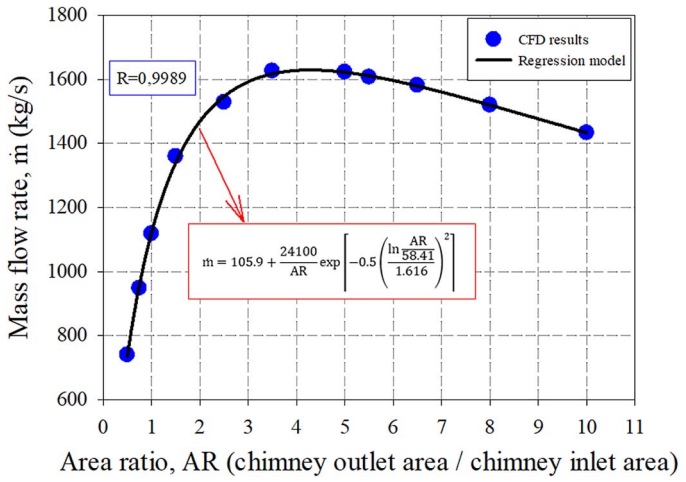

Figure 10. *Mass flow rate of air in the system as a function of AR.*

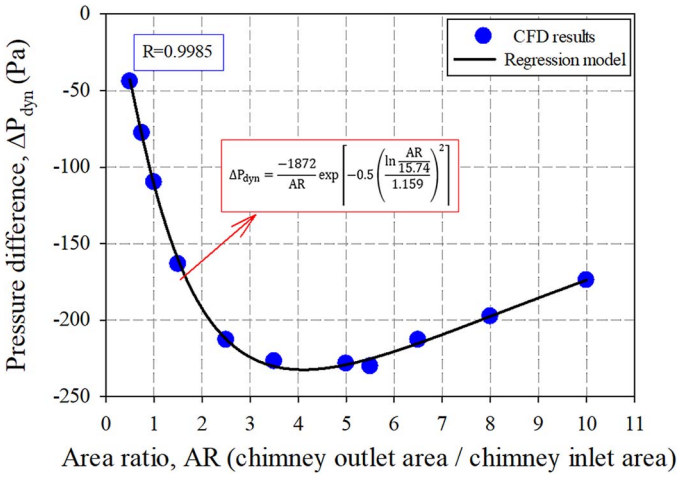

Figure 11. *Dynamic pressure difference across the turbine as a function of AR.*

It is also understood from Figure 14 that there is an optimum region of AR, which can be recommended for the chimney design. The optimum AR is found to be in the range of 3 to 6 for the geometric characteristics of the pilot plant. It is well documented that chimney design covering AR is of vital importance for overall performance assessment [28]. On the other hand, chimney height is a dominant parameter on dynamic pressure difference and mass flow rate figures [29]. From this point of view, it might be useful to consider divergent chimney design along with optimum chimney height. Collector slope is also significant to improve buoyant effects in SCs [30]. Therefore, optimum design conditions can be extended to the optimization of slope angle for collector part in the upcoming works.

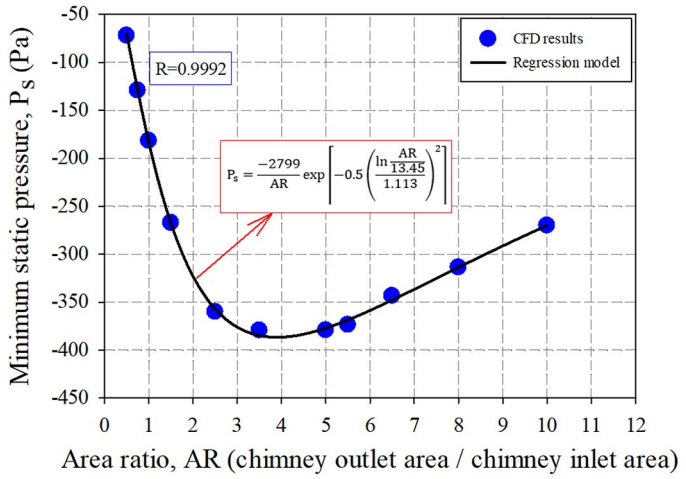

Figure 12. *Minimum static pressure in the plant as a function of AR.*

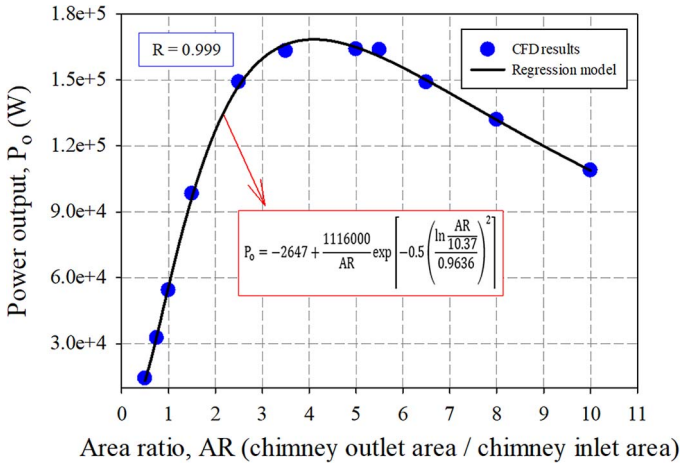

Figure 13. *Power output of the plant as a function of AR.*

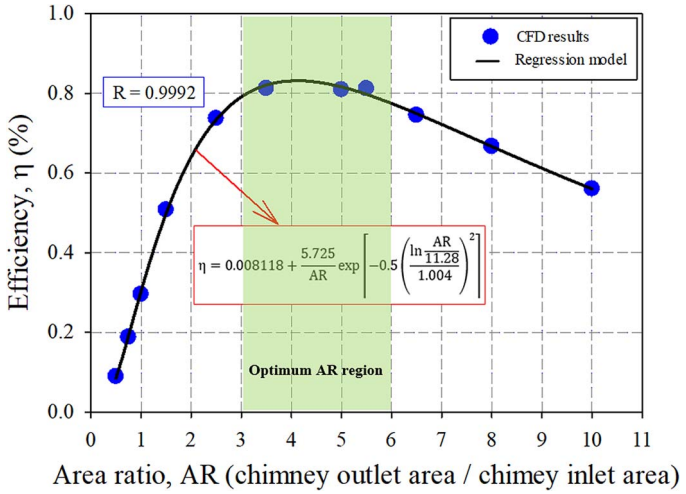

Figure 14. *System efficiency as a function of AR with the optimum AR region.*

3. Highlights

- For AR = 1, $\dot{m}$ = 1122.1 kg/s while it is 1629.1 kg/s for the optimum AR value of 4.
- ΔP_{dyn} = −109.8 Pa for the reference case, whereas it is −232.3 Pa for AR = 4.1.
- Minimum static pressure is −386.6 Pa for the optimum case.
- P_o and η are 54.3 kW and 0.29% for AR = 1.
- P_o and η are enhanced to 168.5 kW and 0.83% for the optimum case.
- AR can be selected from 3 to 6 for the pilot plant.

4. CONCLUSIONS

The influence of AR (the ratio of chimney outlet area to the chimney inlet area) is comprehensively analysed through a justified CFD methodology by taking the geometric characteristics of MPP into consideration. AR is studied as an independent variable in the research to be able to cover both concave and convex chimney designs (0.5–10). Following the accuracy verification of the CFD results and mesh-independent solution, main performance-related parameters are evaluated as a function of AR such as temperature, pressure and velocity distribution within the plant, temperature rise of air in collector, mass flow rate of air around the turbine section, dynamic pressure difference across the turbine, minimum static pressure within the plant, power output and system efficiency. The following bullet points can be achieved through the research:

- For the AR = 0.5, the greatest air temperature at the collector outlet is achieved with 314.9 K. T_a is found reducing up to a certain value of AR, which is 3.75. For this point, minimum temperature increase is obtained for air with 305.2 K.
- For the reference chimney design (AR = 1) maximum air velocity around the turbine position is found as 13.9 m/s for the solar intensity of 1000 W/m^2. On the other hand, Maximum V_a is determined to be 19.1 and 19.8 m/s for the AR of 2.5 and 5, respectively.
- Mass flow rate of air within the plant is a key parameter on system performance. $\dot{m}$ is found to be 1122.1 kg/s for the reference geometry (AR = 1) of MPP. However, for an optimum geometry, which corresponds to an AR value of about 4, $\dot{m}$ is achieved to be 1629.1 kg/s, which needs to be noted.
- Dynamic pressure difference across the turbine is determined to be −109.8 Pa. This parameter directly affects the power output of any SCPP, hence any potential improvements in this figure enhance both power output and system efficiency. ΔP_{dyn} is obtained to be −232.3 Pa for the optimum AR value of 4.1.
- Minimum static pressure within the plant usually takes greater values compared to ΔP_{dyn}. This is a performance indicator for the limit case, and P_s is given to be −386.6 Pa for the optimum case.
- The optimum value of AR, which maximizes the power output and system efficiency, is obtained to be 4.1 for MPP.

- P_o and η are achieved to be 54.3 kW and 0.29% for the reference geometry of MPP (AR = 1). However, for the optimum value of AR (4.1), the aforesaid performance parameters are observed to be 168.5 kW and 0.83%, which proves the practicality of divergent chimney design.
- In further works, thin film photovoltaic (PV) modules can be considered in SCPPs as chimney wall element, and the tilt angle, in other words, AR of divergent chimney can be also optimized in terms of most efficient cooling strategy of PV cells for better thermodynamic performance figures from the entire plant.

REFERENCES

[1] Sen H, Cuce E. Dynamic pressure distributions in solar chimney power plants: A numerical research for the pilot plant in Manzanares, Spain. *WSSET Newslett* 2020;**12**:2–2.

[2] Cuce E, Cuce PM. Performance assessment of solar chimneys: Part 1—impact of chimney height on power output. *Energ Res J* 2019;**10**: 11–9.

[3] Cuce E, Cuce PM. Performance assessment of solar chimneys: Part 2—impacts of slenderness value and collector slope on power output. *Energ Res J* 2019;**10**:20–6.

[4] Kumar P, Agrawal A. A noble approach for the clean energy generation: solar updraft tower. In *In: Proceedings of the International Conference on Sustainable Energy and Environmental Challenges (SEEC)*. 26–27 February 2017. Mohali, India.

[5] Haaf W, Friedrich K, Mayr G, Schlaich J. Solar chimneys part I: principle and construction of the pilot plant in Manzanares. *Int J Solar Energ* 1983;**2**:3–20.

[6] Haaf W. Solar chimneys: part II: preliminary test results from the Manzanares pilot plant. *Int J Sust Energ* 1984;**2**:141–61.

[7] Mullett LB. The solar chimney overall efficiency, design and performance. *Int J Ambient Energ* 1987;**8**:35–40.

[8] Karimipour FP, Hamid BH. Performance enhancement and environmental impact analysis of a solar chimney power plant: twenty-four-hour simulation in climate condition of Isfahan province, Iran. *Int J Eng* 2017;**30**:1260–9.

[9] Fathi N, Aleyasi SS, Vorobieff P. Numerical–analytical assessment on Manzanares prototype. *Appl Thermal Eng* 2016;**102**:243–50.

[10] Abdelmohimen MAH, Algarni SA. Numerical investigation of solar chimney power plants performance for Saudi Arabia weather conditions. *Sust Cities Soc* 2018;**38**:1–8.

[11] Larbi S, Bouhdjar A, Chergui T. Performance analysis of a solar chimney power plant in the southwestern region of Algeria. *Renew Sust Energ Rev* 2010;**14**:470–7.

[12] Li J, Guo H, Huang S. Power generation quality analysis and geometric optimization for solar chimney power plants. *Solar Energ* 2016;**139**: 228–37.

[13] Ngala GM, Oumarou MB, Muhammad AB, Shuwa M. Evaluation of solar chimney power plant in semi-arid region of Nigeria. *Arid Zone J Eng Technol Environ* 2015;**11**:1–12.

[14] Tinghzen M, Wei L, Guoliang X. Analytical and numerical investigation of the solar chimney power plant systems. *Int J Energ Res* 2006;**30**:861–73.

[15] Li J, Guo P, Wang Y. Effects of collector radius and chimney height on power output of a solar chimney power plant with turbines. *Renew Energ* 2012;**47**:21–8.

[16] Choi YJ, Kam DH, Park YW, Jeong YH. Development of analytical model for solar chimney power plant with and without water storage system. *Energy* 2016;**112**:200–7.

[17] Toghraie D, Karami A, Afrand M, Karimipour A. Effects of geometric parameters on the performance of solar chimney power plants. *Energy* 2018;**162**:1052–61.

[18] Hassan A, Ali M, Waqas A. Numerical investigation on performance of solar chimney power plant by varying collector slope and chimney diverging angle. *Energy* 2018;**142**:411–25.

[19] Hu S, Leung DYC, Chen MZQ. Effect of divergent chimneys on the performance of a solar chimney power plant. *Energ Proc* 2017;**105**:7–13.

[20] Koonsrisuk A, Chitsomboon T. Effect of tower area change on the potential of solar tower. In *The 2nd Join International Conference on Sustainable Energy and Environment (SEE)*. 21–23 November 2006. Bangkok, Thailand.

[21] Zandian A, Ashjaee M. The thermal efficiency improvement of a steam Rankine cycle by innovative design of a hybrid cooling tower and a solar chimney concept. *Renew Energ* 2013;**51**:465–73.

[22] Dhahri A, Omri A, Orfi J. Numerical study of a solar chimney power plant. *Res J Appl Sci Eng Technol* 2014;**8**:1953–65.

[23] Bayareh M. Numerical simulation of a solar chimney power plant in the southern region of Iran. *Energ Equipment Syst* 2017;**5**:431–7.

[24] Kalantar V, Zare M. Simulation of flow and heat transfer in 3D solar chimney power plants-numerical analysis. In *Jordan International Energy Conference (JIEC)*. 20–22 September 2011. Amman, Jordan.

[25] Ming T, Richter RK, Meng F *et al.* Chimney shape numerical study for solar chimney power generating systems. *Int J Energ Res* 2013;**37**:310–22.

[26] Rabehi R, Chaker A, Aouachria Z, Tingzhen M. CFD analysis on the performance of a solar chimney power plant system: case study in Algeria. *Int J Green Energ* 2017;**14**:971–82.

[27] Das P, Chandramohan VP. CFD analysis on flow and performance parameters estimation of solar updraft tower (SUT) plant varying its geometrical configurations. *Energ Sources A Recov Utiliz Environ Effect* 2018;**40**:1532–46.

[28] Cuce E, Sen H. Dünden bugüne güneş bacası güçsantralleri: sistem güççıkışına etki eden performans parametreleri. In *Avrasya 7. Uygulamalı Bilimler Kongresi*. 21–22 August 2020. Trabzon, Turkey.

[29] Cuce E, Sen H, Cuce PM. Numerical performance modelling of solar chimney power plants: Influence of chimney height for a pilot plant in Manzanares, Spain. *Sust Energ Technol Assess* 2020;**39**:100704.

[30] Cuce E. Güneş bacası güçsantrallerinde toplayıcı eğiminin çıkış gücüne ve sistem verimine etkisi. *Uludağ Üniv Mühendislik Fakült Dergisi* 2020;**25**:1025–38.